# Behaviour of concrete specimens retrofitted with bio-based polyurethane coatings under dynamic loads

H.M.C.C. Somarathna [a,b,1,*], S.N. Raman [c,2,*], D. Mohotti [d], A.A. Mutalib [b], K.H. Badri [e]

[a] Department of Civil Engineering, Faculty of Engineering, University of Jaffna, Ariviyal Nagar, Killinochchi 44000, Sri Lanka
[b] Department of Civil Engineering, Faculty of Engineering and Built Environment, Universiti Kebangsaan Malaysia, 43600 UKM Bangi, Selangor, Malaysia
[c] Civil Engineering Discipline, School of Engineering, Monash University Malaysia, Jalan Lagoon Selatan, 47500 Bandar Sunway, Selangor, Malaysia
[d] School of Engineering and Information Technology, The University of New South Wales, Canberra, ACT 2600, Australia
[e] Department of Chemical Sciences, Faculty of Science and Technology, Universiti Kebangsaan Malaysia, 43600 UKM Bangi, Selangor, Malaysia

## HIGHLIGHTS

- Elastomeric bio-based PU resins were prepared and coated on concrete.
- The dynamic responses of bare and PU coated concrete specimens were examined.
- Strength, strain during ultimate failure, and strain energy density were enhanced.
- Drastic fragmentation effects can be reduced.

## ARTICLE INFO

## ABSTRACT

Experimental investigation was conducted using concrete specimens to assess the effectiveness of bio-based polyurethane (PU) coating synthesized from palm kernel oil in enhancing the dynamic mechanical response of concrete specimens under quasi-static and dynamic loads. The dynamic loading condition was simulated by conducting three-point bending tests at a strain rate of 0.067 s$^{-1}$, and simultaneously, under quasi-static loading (strain rate of 0.00033 s$^{-1}$) conditions. The application of PU layer(s) (either on the impact face, rear face, or on both faces of the concrete specimens) increases the dynamic resistance of the concrete element, which can be enhanced by increasing coating thickness on either face of the concrete element. Under dynamic conditions, with 10% of total coating thickness compared to the beam depth, strain during ultimate failure, and strain energy density were enhanced significantly with marginal enhancement in the ultimate flexural strength. PU coating does not debond during ultimate failure of the test specimens which implies good adhesion characteristics, and even with minimum coating thickness (2.5%), drastic fragmentation effects can be reduced. Bio-based PU is a green material and application of PU coating provides a viable and sustainable technique for protecting concrete structures against dynamic loads.

© 2020 Elsevier Ltd. All rights reserved.

## 1. Introduction

Repair and strengthening of building elements and other infrastructure against dynamic loads, from low velocity impact to high impulsive loads, has received renewed interest among researchers following the increase in failures of these structures under dynamic loads over the past few decades [1,2]. Typical examples for low velocity impacts are vehicle accidents (e.g., impact generated during the accidents in car parks on columns and sideways of roads); direct human action (e.g., impact of objects when dropped, impact of thrown objects, and accidental impact in the

process of being moved); impact generated during falling and swinging of objects in industries; low scale explosion in factories; impact of falling objects during earthquake; impact of flying debris or objects generated by explosions; impact of debris bring by natural disasters such as flood, tsunami and tornado; impact on the marine and offshore structures exposed to ship and ice impact etc. In addition, loading can be severe as high impulsive loadings such as direct blast and ballistic loadings. Generally impact loads generate very high intensity load and pressure within short time duration which results high strain rate, stress wave on elements, and significant inertial effect, thus leading to a dynamic structural response that is differ from the quasi-static response of structure [3]. These events produce a wide spectrum of response and destruction to the target, and internal damages which is caused by these impact loads is sometimes undetectable and may result the reduction in load carrying capacity of the structure, and severe damage may result a catastrophic failure of the structure. The severity of these destruction is governed by the several aspects such as mass and shape of the impactor, velocity of impact, the weight of the explosive material and the stand-off distance to the target, type of composite structures and systems, and type of structural material used. Therefore, proper attention should be paid to the structural material to reduce the level of destruction [3,4].

Although cementitious materials are known to be rigid, they fail via tensile cracking when overloaded and subjected to dynamic loads, because they have low tensile strain capacity (with tensile strain of approximately 0.0001, nearly one-tenth that of compressive strain), lower fracture toughness of approximately 0.01 kJ/m$^2$ compared with other structural materials such as mild steel (100 kJ/m$^2$), and are brittle [5,6]. Therefore, the concrete member may suffer brittle shear failure in addition to the flexural failure even though they were designed to fail in flexural failure. Several techniques, mostly composite laminates such as fibre-reinforced polymer (FRP) composites and its variants [7-19], and cementitious composites [20-24] have been used to retrofit concrete and other civil structures against a wide range of loading conditions. However, their limitations under dynamic loads have led to the search for novel, feasible, and sustainable techniques to strengthen concrete structures and other structural elements [3,25]. Evidences from the past work indicate that enhancing strain and energy absorption capacities of structural elements can substantially reduce damage and fragmentation effect under dynamic loads, including under high impulsive loading conditions [3,26,27]. The application of materials with high stiffness and high strain capacity is a highly effective mean to enhance the energy absorption capacity of structural elements [3,25-30]. One of the novel approaches to mitigate the destructive effects of dynamic loads is the application of elastomeric coatings to protect structures [3,25,29,31-38]. Numerous studies have been conducted to investigate the possibility of using these coatings as a technique for structural strengthening because they appear to have potential to significantly enhance the resistance of structures against dynamic loads [26,29,33-35,39-44].

The first attempt to use elastomeric polymer under dynamic and impulsive loads was undertaken by the US Air Force Research Laboratory at the Tyndall Air Force Base to evaluate the applicability of 21 types of polymers, including 14 elastomeric polymers, in enhancing the structural performance of masonry structures under blast effect [29,34,35]. These investigations deduced that elastomeric polymers significantly enhanced the resistivity of structures under such loads. In particular, although masonry walls had failed, applying coatings of elastomeric polymers, and their variants, prevented fragmentation, which was a major cause of injury among the occupants of structures [29,34,35]. These polymers behave like a membrane by stretching, thereby minimizing the incidents of flying debris upon impact and resulting in causalities [3,25,26,29,35]. In addition, the use of elastomeric polymers provide better solutions than conventional and advanced tech-

niques; hence, it is cost-effective (low capital cost and low resource consumption) and applicable to existing structures [3]. The succeeding studies that apply this technique have shown that elastomeric polymers are effective in dynamic protection of other types structural materials such as masonry [45-48], metals [28,33,40-43,49-51] and composites [38,39,44,52-55]. Although concrete is the most widely used structural material, research on the use of elastomeric polymer coatings to strengthen concrete structures has been limited. Only a limited number of studies investigating the effect of elastomeric polymers on the dynamic (blast) resistance of concrete structures have been published, because controlled laboratory-scale experiments remains challenging. Raman et al. [5,26,56] investigated the effect of elastomeric polyurea on the impulsive response of reinforced concrete panels by conducting field blast tests. Parniani and Toutanji [57] studied the fatigue and monotonic behaviour of concrete beams strengthened with a polyurea coating system. Iqbal et al. [58] investigated the applicability of polyurea coatings for enhanced blast survivability of concrete. Findings of these studies indicated that application of elastomeric polymer improves the flexural capacity as well as ductility of reinforced concrete elements. However, it is progressing rapidly given the outstanding mechanical behaviour and positive effects of elastomeric polymers on other types of structural materials.

Among numerous polymers, Polyurethane (PU) and its variants have been receiving increased attention from researchers and engineers because of their suitable and customisable structural property, which is correlated with a number of physical and mechanical properties, including high flexibility, elasticity, and resistance to impact, abrasion, and weather [3,25,27]. The mechanical properties of PU is highly dependent on the types and content of the polyols and diisocyanates used in the synthesis [25,59], and applied loading condition [27,32,60,61]. PU is an inexpensive, light-weight, soft, and abrasion-resistant retrofit for most structural materials, such as masonry, metal, concrete, and other composites. It can be easily applied using simple techniques, such as spraying, brushing, bar coating, and pouring. PU readily adheres to surfaces and rapidly cures [3,25].

A series of studies undertaken by the authors [32,59-64] suggest that bio-based PU synthesized from palm kernel oil is an alternative sustainable coating material that can be used to enhance the dynamic resistance of structural elements, in its place for petroleum based elastomeric polymers used in recent researches. The present study was undertaken to analyse the applicability and effectiveness of bio-based PU coating under dynamic loads at laboratory scale with polymer coated and uncoated concrete beam specimens. In the current work, attention has been paid to investigate its behaviour under dynamic condition which can be generated from an event of impact. To evaluate the efficiency of the proposed retrofitting technique, cast (unreinforced) concrete specimens were used and coated with 10 different configurations, which were combinations of various thicknesses and coating arrangements. The specimens were subjected to loading of two different strain rate regimes, simulating quasi-static and impact conditions. The experimental method allows the assessment of responses in terms of the enhancement of strength, energy absorption, flexibility, and fracturing of PU-coated concrete specimens.

## 2. Experimental programme

### 2.1. Materials

#### 2.1.1. Concrete

Commercially available ordinary Portland cement (CEM-I) with a strength class of 42.5 N, was used in this study. The density of the

cement was 3160 kg/m$^3$, and its quality complied with the ACI 211 [65]. Locally available river sand was used as fine aggregate, with a maximum size of 5 mm. The sand was clean and nearly free of debris. The specific gravity and fineness modulus of the fine aggregate were 2.61 and 2.70, respectively. The coarse aggregate used in this study was locally sourced from 9.5 mm downgrade crushed stones. The specific gravity and fineness modulus of the coarse aggregate were 2.65 and 5.93, respectively. Fig. 1 shows the plot for the grading curves of the fine and coarse aggregates. Both types of aggregates were air-dried; therefore, free moisture on the surface of the aggregates was assumed negligible.

The concrete grade considered in this investigation was 30 MPa for cylinders. The concrete mix designs used in this study are listed in Table 1. Table 2 provides the average strength values of the cubes and the cylinders for the 7th, 14th, and 28th day compressive strength of the used concrete mix. In the investigation, 150 mm × 150 mm × 150 mm cube specimens and 100 (D) mm × 200 (H) mm cylindrical specimens were used. The characteristic compressive strength of the specimens was calculated based on ASTM C-39 [66].

### 2.1.2. Polyurethane

Palm-based polyol (PKO-p) [67] was supplied by the Polymer Research Centre (PORCE) of the Universiti Kebangsaan Malaysia. 4,4-diphenylmethane diisocyanate (MDI) was obtained from Cosmopolyurethane Sdn. Bhd., Malaysia. Acetone (industrial grade) and polyethylene glycol (PEG: Mw 200 Da) were sourced from Sigma Aldrich (M) Sdn. Bhd., Malaysia. The synthesis of bio-based PU elastomer was undertaken from the rapid reaction of PKO-p and MDI via pre-polymerization in the presence of PEG as a plasticizer, and without any catalyst under ambient temperature. The mix proportion of the PKO-p: MDI: PEG was used as 100:80:6 (by weight) which was obtained based on the experimental investigations conducted by authors [27,32,59-62,64]. Acetone was added based on the total weight of each system separately with the same percentage of 35% w/w.

### 2.2. Preparations of concrete specimens coated with Polyurethane.

The concrete specimens were prepared using predesigned moulds (Fig. 2). All the moulds were oiled first and then placed on the vibrating table. Concrete was mixed uniformly in the mixer according to the mix design specified in Table 1; fresh concrete was then poured into the moulds. Concrete was evenly compacted using a mechanical table vibrator until no bubble was present on the surface. To ensure an even top surface, concrete was finished very carefully using a steel trowel. The prepared concrete test specimens with a dimension of 160 mm (L) × 40 mm (W) × 40 mm (T) were removed from the moulds after 1 day of casting and placed in a water tank to ensure proper curing. All the specimens were water-cured for 7 days at ambient temperature. After 7 days, the specimens were further air-cured at ambient temperature. The uncoated specimen was designated as CON, as shown in Fig. 3. A total of 10 different types of coating configurations were used throughout the study, albeit with variations in coating thickness. Table 3 presents the schematic diagrams of the bio-based PU coated concrete sample arrangements used in this study. Different configurations were produced by applying PU coatings with varying thicknesses on the top and bottom faces of the moist-cured concrete test specimens. The determined strength would depend on the preparation, moisture condition, and curing condition; hence, the same materials, techniques, and conditions were used during the preparation of the test specimens.

All the concrete specimens were set aside for a few hours to achieve a dry surface before coating. PU was fully coated onto the surfa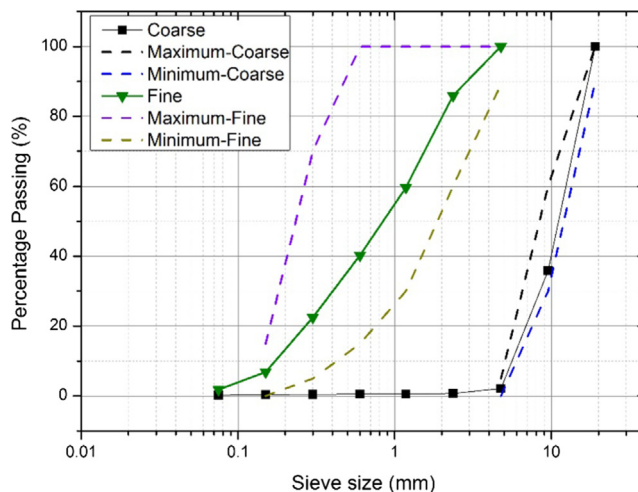ce, and no additional adhesive was used, since PU is a self-adhesive polymer on concrete. As shown in configurations T1, T2, and T4, 1, 2, and 4 mm-thick PU coatings were applied on the impact-facing surface (top face during testing), with 2.5%, 5%, and 10% PU layer thickness, respectively, compared with the thickness of the uncoated concrete specimen. Fig. 4(a) shows the sample T4, which is coated with 4 mm-thick PU layer on the top face of the concrete specimen. Similarly, B1, B2, and B4 were all coated on their bottom face during testing (rear face compared with impact face) with similar coating thicknesses as aforementioned. Configurations T1B1, T2B2, and T4B4 were formed from the combination of T1, T2, and T4 with B1, B2, and B4, respectively, by coating both sides with 1, 2, and 4 mm-thick PU.

### 2.3. Dynamic flexural test

Three point bending test was conducted according to the ASTM C-293 [68] standard using Zwick 100 kN Proline Materials Testing Machine (Zwick Roell AG, Ulm, Germany), model no. Z100 (Fig. 5), under displacement-controlled conditions at different strain rates (different crosshead speeds were used to attain varying strain rates). All the specimens were tested on the same day after casting and coating to approximately maintain the same age of the specimens. The length of the test span was 120 mm, which was thrice its depth as tested, thereby allowing sufficient overhang (20 mm) on each end to avoid slipping through the support. The length of the test span was checked before testing each specimen to verify
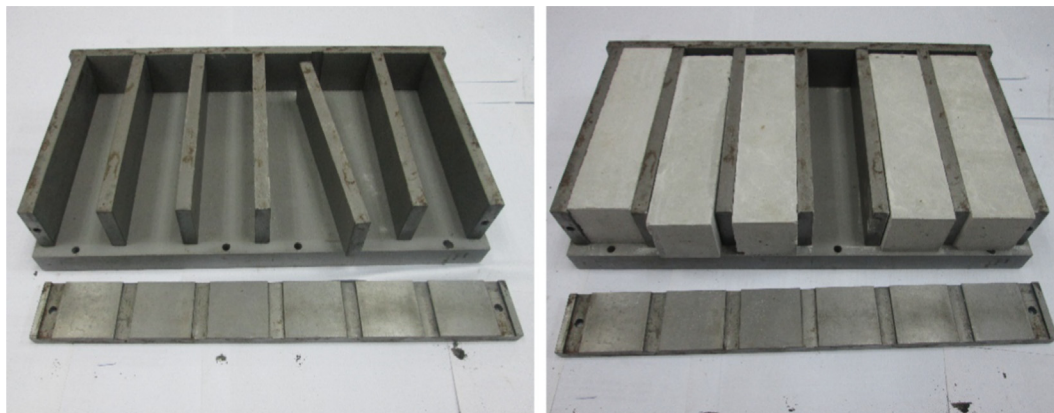


**Fig. 1.** The grading curve of the fine aggregate and coarse aggregate.

**Table 1**
Details of mix design proportions for the grade 30 concrete produced in the experimental study.

| Constituent materials | Quantity (kg/m$^3$) |
|---|---|
| Cement | 380 |
| Fine aggregate | 640 |
| Coarse aggregates | 1190 |
| Water | 190 |

**Table 2**
Details of cube and cylinder average compressive strengths of the concrete mix used.

| Age | Average compressive strength | |
|---|---|---|
| | Cube strength (MPa) | Cylinder strength (MPa) |
| 7 days | 32.18 | 24.41 |
| 14 days | 38.66 | 28.85 |
| 28 days | 42.28 | 32.12 |

**Fig. 2.** Pre-designed moulds used to cast concrete specimens.



**Fig. 3.** Uncoated concrete specimens (Control (CON)).

that it was within 2% of the accurate span length. The test specimens were turned on their side with respect to their position as they were moulded and centred on the support blocks (Fig. 5). All the test specimens were tested at ambient temperature, with crosshead speeds of 200 mm/min and 1 mm/min to obtain 0.067 s$^{-1}$ and 0.00033 s$^{-1}$ strain rate conditions, which corresponded to impact and quasi-static conditions, respectively. Two sets of experimental setups, denoted by low (L) and high (H), were used to characterise the responses under quasi-static and impact conditions. Actuator displacement was controlled using a computer with the testing software testXpert II (Zwick Roell AG, Ulm, Germany). The operation and data acquisition (time, load, and mid-span deflection) of the testing system were undertaken. The test was continued until the ultimate failure of the test specimens occurred. The time history of the force transmitted through the samples and the deflection at the midpoint of the sample were measured. In addition, strain energy density is correlated with the ductility of a test specimen. Cumulative strain energy was computed by integrating the area underneath the stress–strain curve. The maximum flexural stress, failure strain, and strain energy density were obtained as the average of six readings. The nature of a crack and its patterns on the test specimens were observed and recorded in situ after each test. Similarly, any damage sustained by the PU coatings was recorded through visual observations.

The actual strain rate was calculated using the time–deflection histories of all the specimens. The plots of the actual strain rate versus the strain of the selected specimens under varying strain rates are shown in Fig. 6; these plots are representative of those of the other specimens with same strain rate condition. The actual

strain rate versus strain histories of the low-strain rate (0.00033 s$^{-1}$) demonstrates a consistent pattern while varying between 0.00029 s$^{-1}$ and 0.00036 s$^{-1}$ (Fig. 6), which can be neglected. The initial region of the curve for the strain rate of 0.067 s$^{-1}$ exhibits an increment from 0 to 0.067 s$^{-1}$ at the beginning of the test because the specimens require $\approx$1 s to reach dynamic equilibrium, which corresponds to a strain rate of 0.067 s$^{-1}$ for all the test specimens. Therefore, the initial stiffness region of these 0.067 s$^{-1}$ strain level curves present a behaviour under a strain level that is slightly lower than that at nearly up to 1 s, which corresponds to a strain of approximately 0.024. Subsequently strain rate fluctuated between 0.063 s$^{-1}$ and 0.068 s$^{-1}$ after reaching dynamic equilibrium (after strain of 0.024) under impact (0.067 s$^{-1}$) condition as shown in Fig. 6.

## 3. Experimental results and discussion

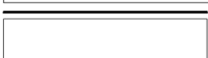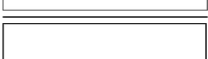A more comprehensive experimental investigation is required to completely understand the effect of coating on the dynamic response and fracture resistance of concrete specimens. The effects of PU coating thickness on the impact face (top face), rear face (bottom face) with respect to loading, and on both faces were investigated. The comparisons undertaken are summarised in Table 4, and the details of the method of comparison, and the specimens used are provided.

### 3.1. Coating on the impact face

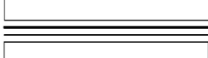This section examines the role of PU coating thickness on the impact face in the efficient dynamic resistance of concrete elements. The behaviours of specimens CON, T1, T2, and T4 are compared and discussed in this section.

As shown in Fig. 7, the mechanical responses of the uncoated concrete samples significantly differ under the two loading conditions tested. Under impact condition, stiffness and ultimate flexural stress are slightly higher than those under quasi-static condition. Moreover, specimen deflection is relatively lower; hence, strain energy is dominant. This occurrence is common among most of the materials and is known as the strain rate effect or strain rate sensitivity; that is, strength values increase whereas strain values decrease under high strain rate condition [6,69]. Johansson [70] reported that the enhancement of strength values could be attributed to two phenomena: viscous (free water) effect and structural (inertia forces and confinement) effect. A viscous effect leads to moderate enhancements, which occur at strain rates of up to 30 s$^{-1}$ (transition zone). By contrast, a structural effect results in a strength enhancement of up to four times the static

**Table 3**
Schematic views of the PU coated concrete sample arrangements used in this study.

| Label on specimen at the test | Specimen designation | Retrofitting scheme | Thickness of PU coating (mm) | |
|---|---|---|---|---|
| | | | Top surface | Bottom surface |
| S1 | CON | | – | – |
| S2 | T1 | | 1 | – |
| S3 | T2 | | 2 | – |
| S4 | T4 | | 4 | – |
| S5 | B1 | | – | 1 |
| S6 | B2 | | – | 2 |
| S7 | B4 | | – | 4 |
| S8 | T1B1 | | 1 | 1 |
| S9 | T2B2 | | 2 | 2 |
| S10 | T4B4 | | 4 | 4 |
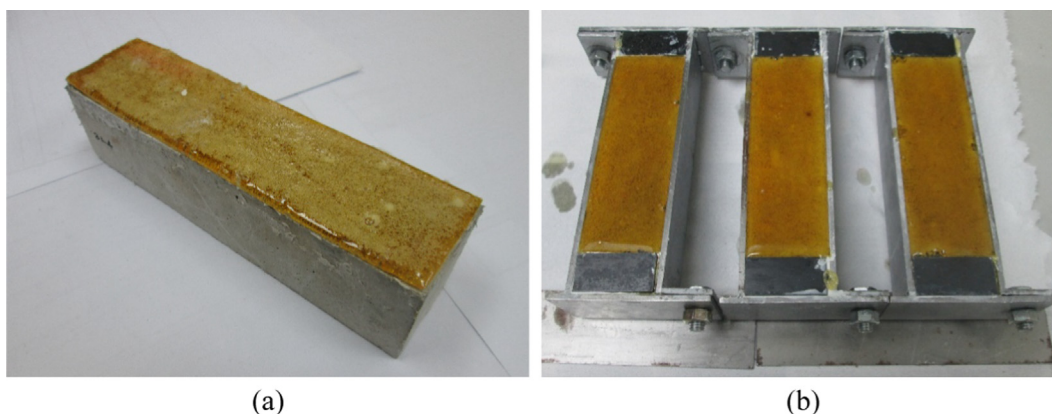


**Fig. 4.** (a) PU coated concrete test specimens (T4) (b) Coating of PU on concrete specimens.

strength when the strain rate is above the transition zone. Eibl and Schmidit-Hurtienne [71] also observed a similar behaviour and described that two mechanisms might govern the strain rate effect at different strain rate regimes. Effects, such as moisture content and cross-aggregate cracks, are assumed to govern strain rate sensitivity at lower strain rates (below $10^{-2}$ s$^{-1}$), whereas inertia effects are assumed to govern the effects of damage formation at higher strain rates (above $10^{-2}$ s$^{-1}$).

Therefore, in the present study, the slight enhancement (5.3%) in the flexural strength of the uncoated concrete specimen may be attributed to the moisture content and cross-aggregate crack effects. In addition, other parameters or combinations of those parameters affect strain rate sensitivity, such as concrete grade, specimen size, test method, and presence of fibres in concrete

[5]. A subsequent experimental study on bio-based PU shows that PU is a highly strain rate-sensitive elastomer, wherein a dramatic transition in behaviour from rubbery to leathery state was observed in response to increasing strain rates [3,27,32,60,61]. In particular, Young's modulus, yield stress, maximum stress, failure stress, as well as resilience and toughness moduli are directly correlated with strain rate, whereas the tangent modulus and failure strain are inversely correlated with strain rate [27,32,60,61]. These findings clearly show that the responses of the coating configurations significantly differ under quasi-static and impact conditions. When PU coating is applied onto the load-receiving face with respect to impact, load and pressure will have to pass through the PU layer before reaching the concrete element. A portion of the energy is absorbed and dissipated through its elastic plastic
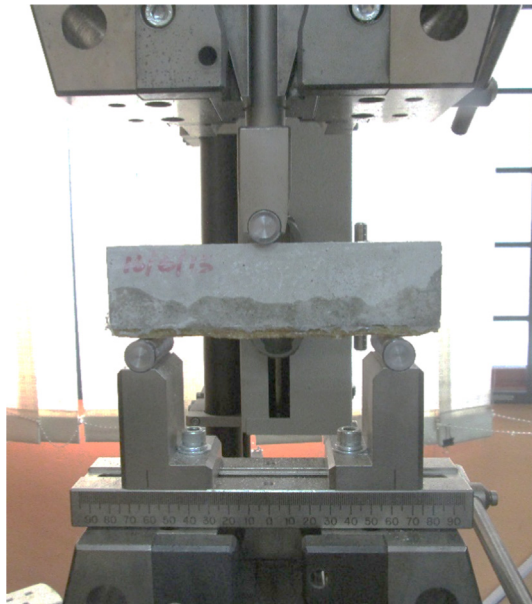
**Fig. 5.** The dynamic flexural test setup.



**Fig. 6.** The actual strain rate-strain curves of test specimens at varying strain rates.

**Table 4**
Summary of the comparisons undertaken using PU strengthened concrete specimens.

| No | Method of comparison | | Specimens used |
|----|----------------------|---------------------------------|----------------|
| 1  | Influence of Coating | Coating on the impact face | CON, T1, T2, T4 |
| 2  | Thickness | Coating on the rear face | CON, B1, B2, B4 |
| 3  | | Coating on the both faces with equal thickness | CON, T1B1, T2B2, T4B4 |

deformation before being transferred to the concrete element. The coating is applied on the compression side; hence, the stiffness of PU significantly increases compared with that under tension, thereby subsequently increasing the amount of absorbed energy. As shown in Fig. 7(a), the stiffness of the PU-coated test specimens decreases with increasing coating thickness under both quasi-static and impact conditions, whereas no significant change in the ultimate flexural stress is exhibited. This finding highlight that the coated specimens exhibit more ductility compared to the uncoated one and ductility is increased with the coating thickness.
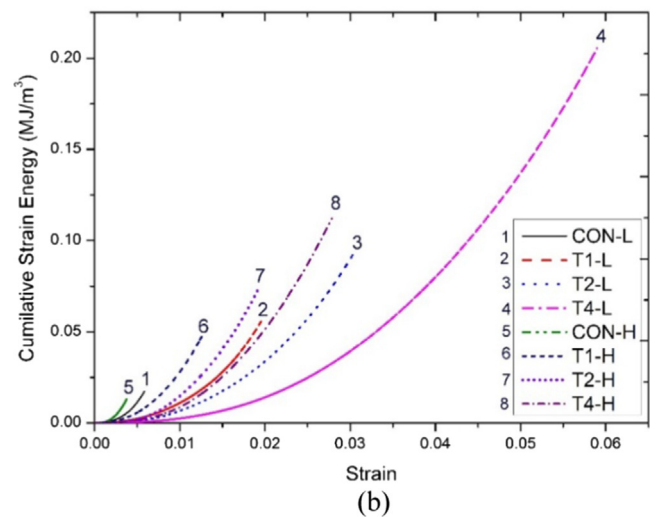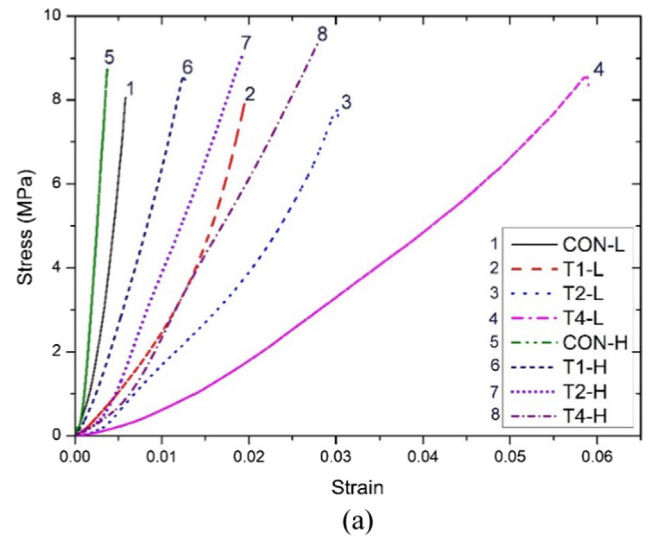




**Fig. 7.** The mechanical responses of the test specimens with top coating (a) stress–strain (b) cumulative strain energy-strain: (T2-L, (T) coating face, (2) coating thickness, (L) strain rate condition).
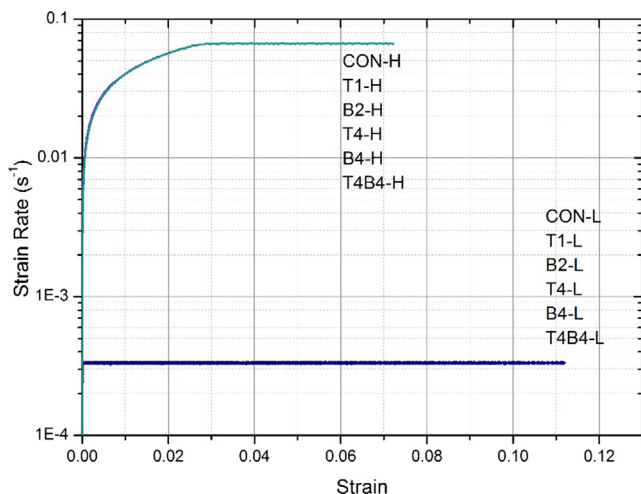
### 3.1.1. Ultimate flexural stress

For all the test specimens in each test configuration, ultimate flexural stress is attained immediately before ultimate failure under both conditions. Fig. 8 (a) presents the average ultimate flexural strength of the studied specimens. Ultimate flexural strength is higher under impact condition than under quasi-static condition for all coating configuration. Under quasi-static condition, a significant difference in ultimate flexural stress is not observed when coating thickness is increased by up to 10% of the thickness (4 mm) of the concrete specimen. Under impact conditions, however, a strength enhancement of 10.3% is exhibited when 4 mm-thick PU coating is applied; moreover, minimal deviations were observed when 1 mm- and 2 mm-thick coatings are applied.

### 3.1.2. Failure strain

When a body is placed under external loads and pressure, internal stresses develop within the body and it will result deformation in the body. If the body is still subjected to external forces and pressure and after gaining ultimate stress of the material, then it begins to cracks and eventually fails. Maximum deflection is the deflection in which occurs just before ultimate failure. Therefore, maximum deflection can also be a measure of the load-carrying capacity of a body. Externally strengthened test specimens exhibit
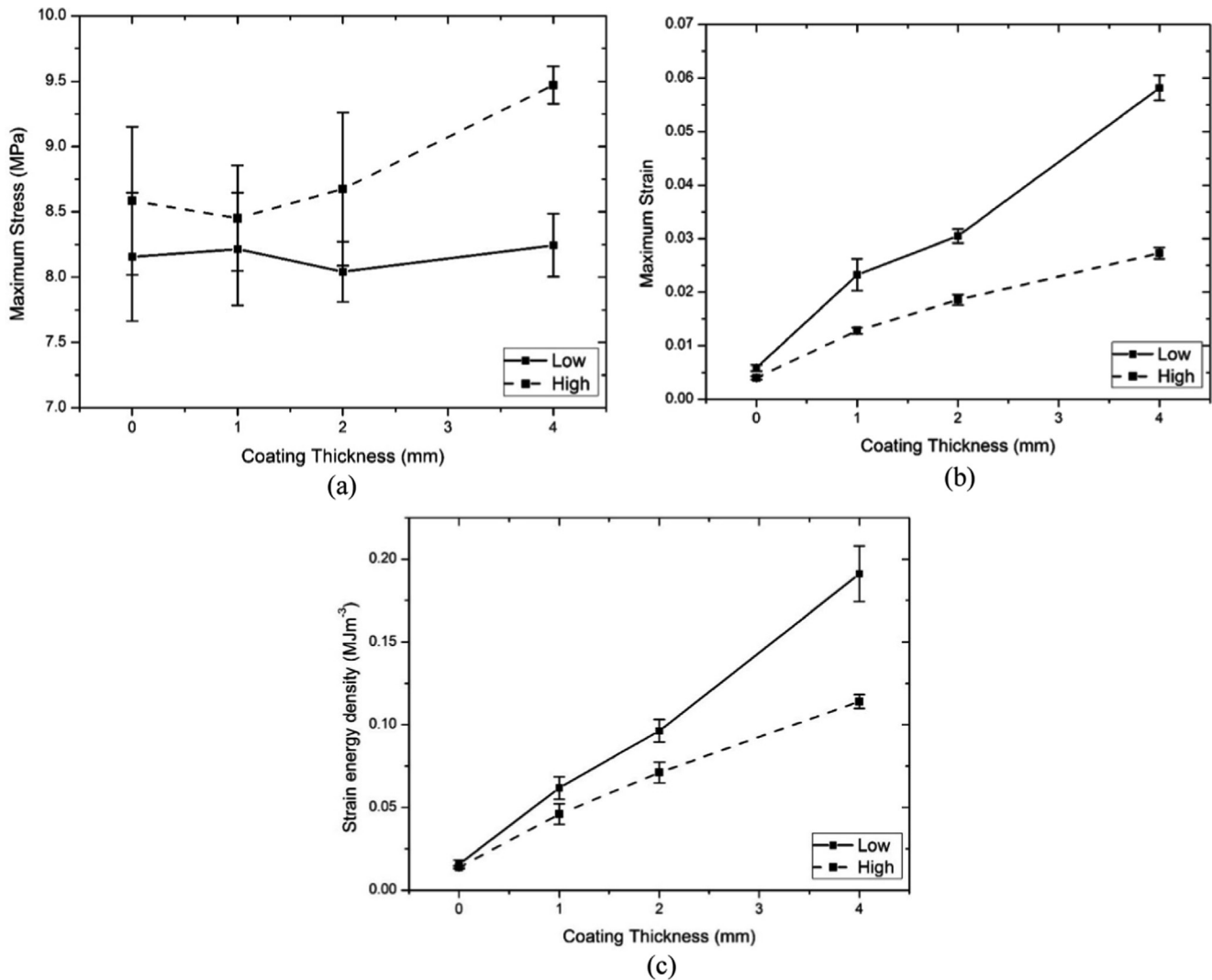
Fig. 8. The flexural properties of the test specimens with top coating; (a) Ultimate flexural stress, (b) failure strain, (c) Strain energy density at failure.

higher strain during ultimate failure because of the elastomeric coating on the impact face, which exhibits high strain capacity. The enhanced strain capacity of the concrete specimens that is attributed to the additional confinement effect is provided by PU. The average strains during ultimate failure are plotted in Fig. 8 (b), which clearly shows that strain during ultimate failure increases significantly with the increasing thickness of the PU layer. Enhancement under impact condition is lower than that under quasi-static condition because of the strain rate sensitivity of both materials [3,26,27,32,60,61].

### 3.1.3. Strain energy density

A common method of comparing dynamic mechanical properties under different load conditions is by considering strain energy during ultimate failure. In addition, strain energy density can be correlated with the ductility of a test specimen. Strain energy can be computed by integrating the area underneath the stress–strain curve [72]. The variation in cumulative strain energy with strain is presented in Fig. 7(b) under both quasi-static and impact conditions. In this research, the strain energy values during ultimate failure are reported by comparing the responses under two test conditions (quasi-static and impact). Strain energy recorded under quasi-static are higher than those recorded under impact, because of the higher failure strain under quasi-static conditions, which

reflect the universal rate sensitive behaviour of most of the materials [5,27,32,60,61,73]. A noticeable increase in strain energy during ultimate failure is observed under both loading conditions. As the thickness of the PU layer increases, the strain energy formed as a result of the enhanced strain work increases linearly with PU layer thickness. Therefore, the strain energy per unit thickness of the PU layer on the impact face can be used as a parameter to quantify the resistance of coated concrete specimens against impact loads. The tested uncoated concrete specimens failed with average strain energy per unit volume of 0.0157 MJ/m$^3$ and 0.0138 MJ/m$^3$ under quasi-static and impact conditions, respectively. All PU-coated concrete specimens failed at higher strain energy density values, which is caused by the enhancement in strain capacity along with coating thickness. Fig. 8(c) shows the plot of the average cumulative strain energy during the ultimate failure of each test specimen. This results clearly show that the presence of a PU layer on the impact face significantly improves the structural capacity and impact resistance of concrete. Therefore, the application of PU coating on the impact face contributed positively to enhancing strain energy in the coated concrete specimens. Evidently, energy dissipation is shared between the concrete and the PU coating, thereby increasing deflection. This finding demonstrates the beneficial contribution of the PU layer in terms of energy absorption. Therefore, the toughness of the

concrete specimens is remarkably improved with the PU coating and subsequently increases with the increasing thickness of the PU layer.

### 3.1.4. Failure mode and crack propagation profile

In terms of cracks during ultimate failure, only flexural cracks were formed and no shear crack was observed (neither diagonal nor direct shear). The crack propagation patterns that formed in the specimens are presented in Fig. 9. In all the cases, except for the uncoated specimen under impact condition, one critical crack existed closest to the mid-span of the concrete specimens. Two major flexural cracks were formed on the uncoated sample under impact condition. These crack lines are stretched across the entire bottom face (Fig. 10). The PU coatings applied on the top face of the concrete specimens were undamaged. This result may be explained by considering the application of loads because coating the impact face (front face) with PU is loaded in compression. When confined PU is loaded during compression, its bulk stiffness increases, thereby attaining good impedance match with the concrete specimen. Debonding was not demonstrated in any specimen. Therefore, the thickness of the PU layer on the impact face does not affect the debonding of PU. The concrete surface was only dusted prior to applying PU coating. The PU material bonded well with concrete even with minimal surface preparation. The crack width on the bottom face of the test specimens was increased with the thickness of the PU coating, which was another co-relative indicator for the maximum deflection (strain) of the specimens. Because, PU coating increases the load carrying capacity of the beam which provide capability to sustain high strains in the tensile face (enhanced flexural capacity) of the beam. Therefore beams can deflect more and when beam fails, it shows wider crack width at the tensile face compared to uncoated sample. Correspondingly, higher coating thickness provide higher enhancement in their flexural capacity, whereas the crack width increases with increasing coating thickness. Meanwhile, more drastic fragmentation effects were observed under impact condition compared with the



(a)



(b)
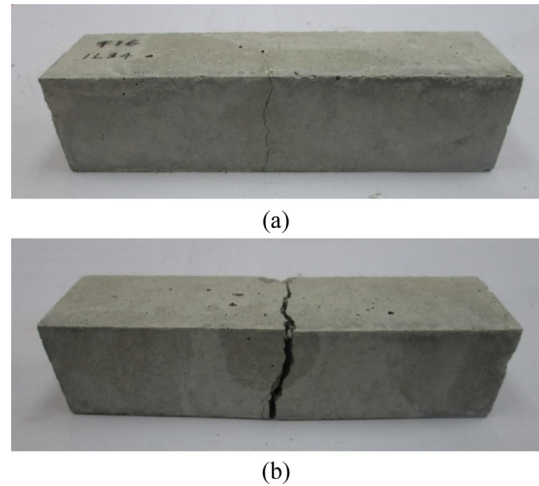
**Fig. 10.** The crack propagation of the control test specimens on bottom face, (a) quasi-static, (b) dynamic.

behaviour under quasi-static condition. The PU coating on the top face significantly enhances the stability level of the concrete element even after the concrete element is cracked. Therefore, an increase in the thickness of the coating on the impact face provides a significant advantage in terms of enhancing resistance against impact loads. An effective protection level can be achieved by controlling coating thickness properly.

### 3.2. Coating on the rear face

This section examines the effect of coating thickness on the rear face on the dynamic resistance of concrete elements. As described earlier, specimens B1, B2, and B4 are similar to T1, T2, and T4, except that the former specimens are coated on their bottom



**Fig. 9.** The crack and crack propagation of the test specimens with top coating (T2-L, (T) coating face, (2) coating thickness, (L) strain rate condition).

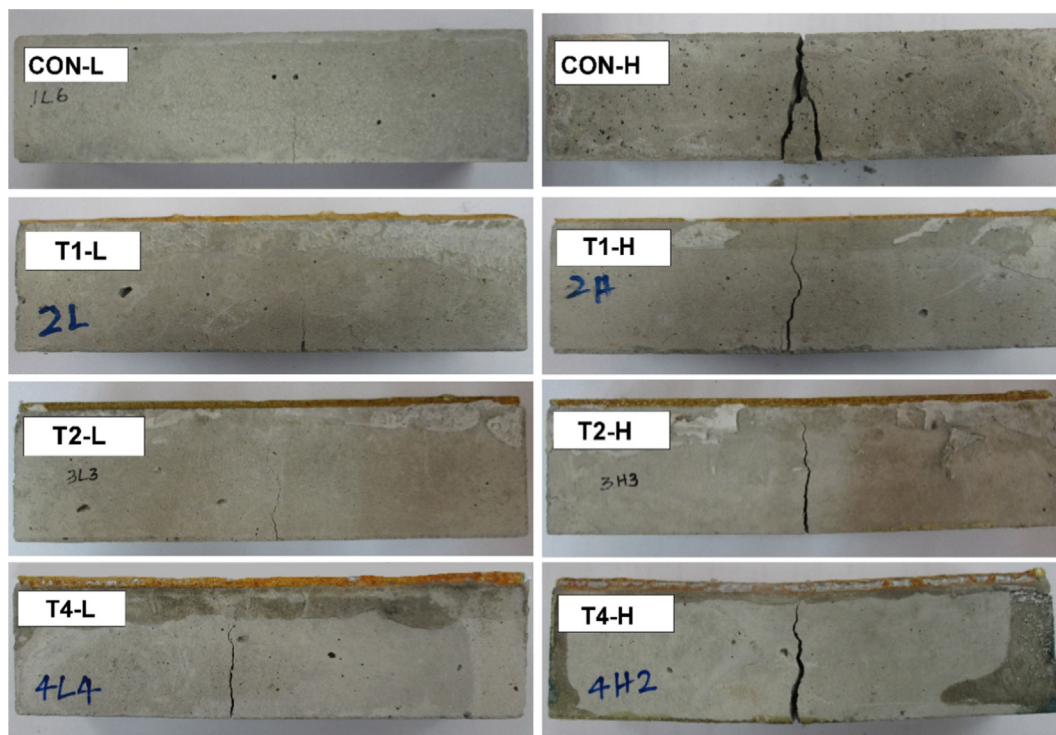surface. Similar to other specimens, B1, B2, and B4 were subjected to two different strain rates (0.00033 s$^{-1}$ and 0.067 s$^{-1}$). However, the dynamic resistance mechanism of these test specimens differs considerably with those of previous specimens. In B1, B2, and B4, loads and pressure will have pass through the concrete element before reaching the PU coating; thereby compressing concrete and increasing stiffness of the concrete, and subsequently, increasing the amount of the absorbed energy by concrete. Part of this energy is transferred to the PU layer which goes under tension. Then, the loads and pressure pass through the PU layer and are reflected on it free face as tensile release waves, thereby significantly decreasing the shear stiffness of the PU, and concurrently, substantially increasing its dissipative capability as a result of its viscoelasticity.

Fig. 11(a) shows the plot of the stress–strain relationship of the coated and uncoated test specimens under quasi-static and dynamic conditions. Similar to the observation in the previous section, higher stiffness and higher ultimate stress were recorded under impact condition compared with under quasi-static condition, whereas specimen deflection is relatively lower. The response of the test element is significantly influenced by the thickness of the PU coating under both test conditions, while an increase in

toughness is demonstrated. The stress–strain responses of the PU-coated concrete specimens under quasi-static condition exhibit an abrupt reduction in flexural strength after gaining reasonable strain with a flexural strength that is approximately equal to the ultimate flexural strength of the uncoated specimen. This finding shows that although the concrete specimen has cracked, PU-coated specimens can still resist load and pressure up to an additional strain level because of the high tensile capacity of PU compared to that of concrete. The additional strain capacity of the coated specimens increases with coating thickness as shown in the stress–strain responses. However, this behaviour was not observed under impact condition, because when concrete beam fails, crack is formed in the tensile face of the beam and subsequently high tensile stress concentration will form in the PU layer along the crack line due to the sudden impact load, and subsequently failure of the PU layer. An important consideration in the dynamic mechanical response of the coated concrete specimens is the increase in failure strain and the enhancement of the total strain energy with respect to the response of the uncoated concrete specimens.

### 3.2.1. Ultimate flexural stress

The stress–strain response showed that the uncoated specimen achieved its ultimate failure immediately after maximum flexural strength under quasi-static condition. By contrast, the ultimate failure was not occurred immediately after maximum flexural strength of PU-coated specimens under quasi-static condition. Generally, ultimate flexural stress occurred immediately before the concrete specimen cracked, though the PU coating is not failed. In coated specimens, although the concrete specimen cracked, the un-failed PU layer could still resist load and pressure up to a significant strain level before it eventually fail. Under impact condition, ultimate flexural stress was attained immediately before failure in all the test specimens in each test configuration. Fig. 12(a) presents the average ultimate flexural strength of the test specimens under both strain rate conditions. The figure clearly shows that the ultimate flexural strength under impact condition is higher than that under quasi-static condition in each coating configuration. This behaviour is similar to that observed when the impact face is coated. Under quasi-static condition, a significant difference was not noticed in the ultimate flexural stress when coating thickness was increased up to 10% of the thickness of the concrete specimen. Under impact condition, however, 4.4% and 10.3% strength enhancement was exhibited for the 2 mm- and 4 mm-thick PU coatings, whereas no enhancement was observed for the 1 mm-thick coating.

### 3.2.2. Failure strain

The maximum deflection and strain energy enhancement among strengthened test specimens imply that the damages sustained by the coated specimens are higher. Similar to the observation in previous section, PU-coated test specimens exhibited higher strain during ultimate failure because of the additional confinement effect on the tension face of the concrete beam. Fig. 12(b) presents the average strains during ultimate failure of different coating configurations under both quasi-static and impact conditions. Under quasi-static condition, enhancements of the failure strain at 6.9, 8.6, and 14.8 times were achieved by specimens B1, B2, and B4, respectively, compared with the uncoated one. Subsequently, failure strain was enhanced by factors of 2.9, 3.3, and 5.2 compared with the uncoated sample under impact condition. Similar to the observation in the previous section, lower strain enhancement was exhibited under impact condition compared with under quasi-static condition because of the strain rate sensitivity of both materials. The enhancement under quasi-static condition is higher than that observed in the previous section with the
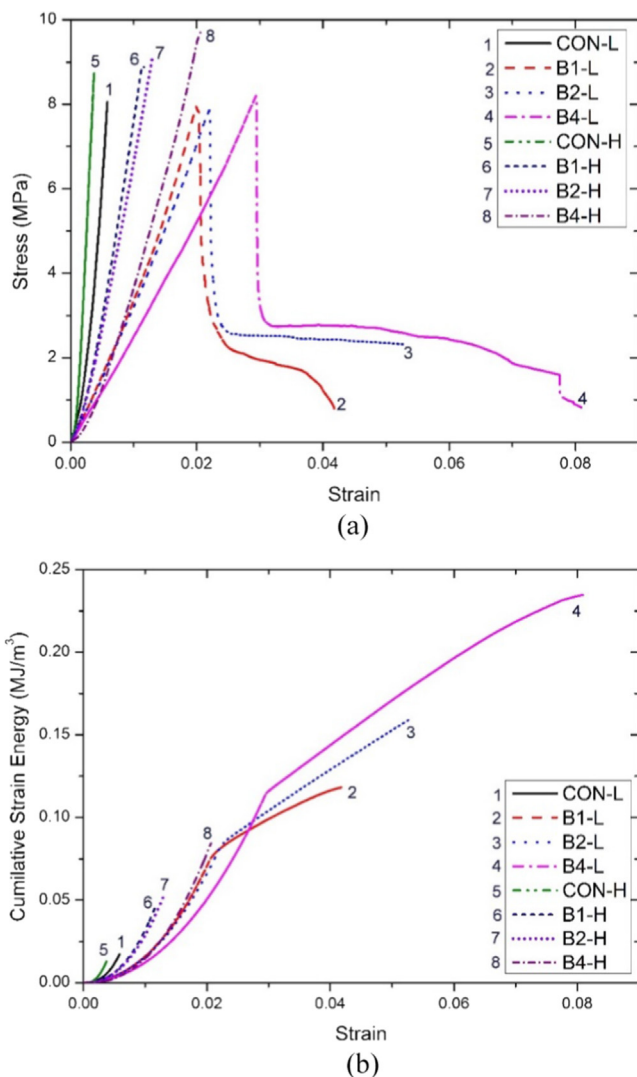


Fig. 11. The mechanical responses of the test specimens with coating on bottom face (a) stress–strain (b) cumulative strain energy-strain: (B2-L, (B) coating face, (2) coating thickness, (L) strain rate condition).
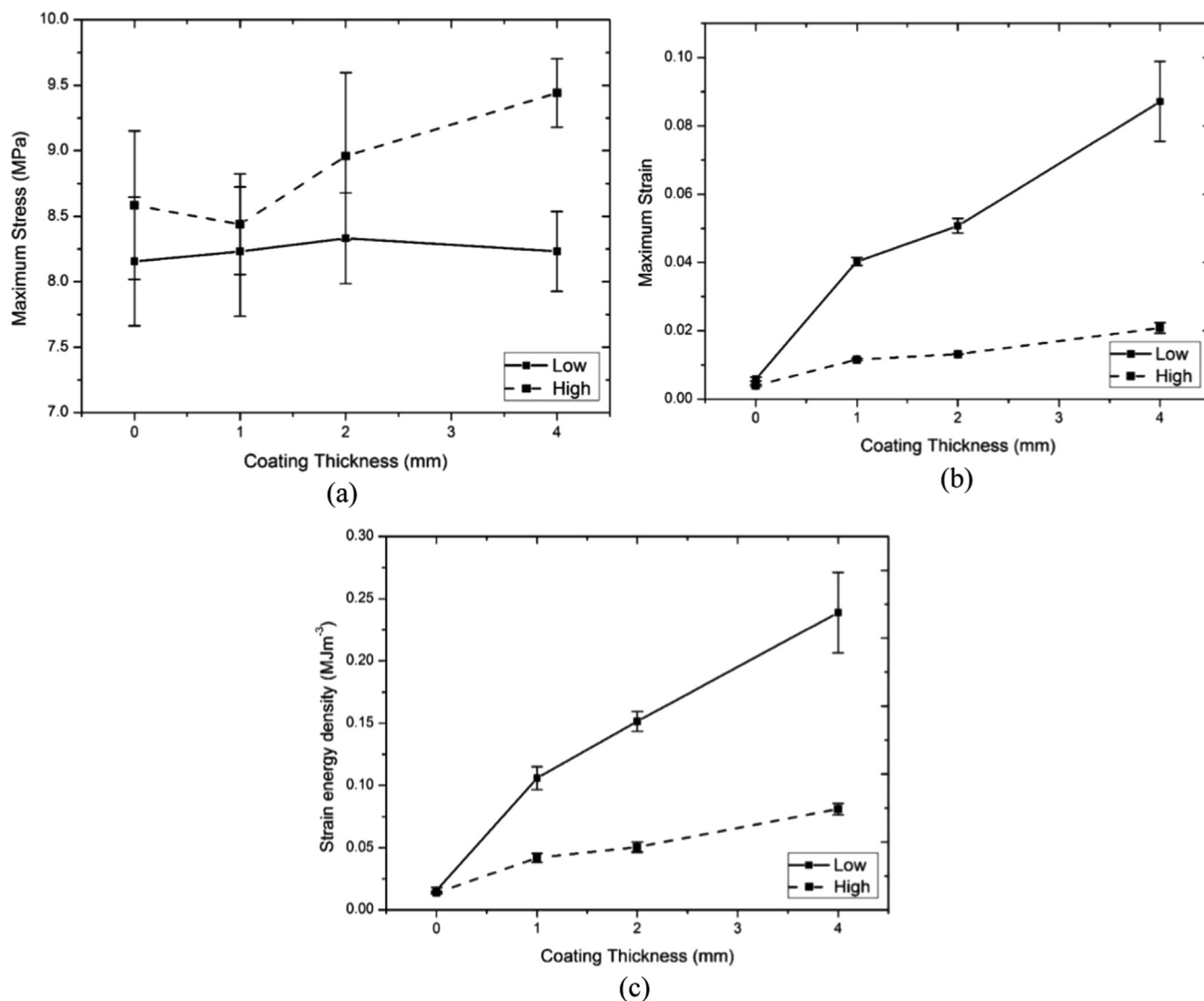
(a)



(b)



(c)

**Fig. 12.** The flexural properties of the test specimens with PU coating on bottom face; (a) Ultimate flexural stress, (b) failure strain, (c) Strain energy density at failure.

same thickness when coated on the impact face. Therefore, the application of PU coating on the impact face contributed positively to enhancing strain energy in the coated concrete specimens. However, enhancement under impact condition is lower than that observed in the previous section. This result implies that coating position is another important criterion that governs the efficiency of dynamic resistance. Though, these findings evidently show that the application of PU coating on the rear face also significantly enhances the strain capacity of concrete elements.

### 3.2.3. Strain energy density

Fig. 11(b) compares the variation of cumulative strain energy with strain under both quasi-static and impact conditions. All the PU-coated concrete specimens exhibited strain capacities higher than that of the uncoated specimen under both loading conditions, which can be attributed to the increase in strain capacity along with coating thickness. The comparison of the average strain energy densities during the ultimate failure of the test specimens with their coating thickness are presented in Fig. 12 (c). Strain energy density increases linearly with PU layer thickness under both quasi-static and impact conditions. This result clearly shows that applying a PU layer on the rear face of the specimens significantly improves the dynamic resistance of concrete. Evidently,

the properties of a concrete element are increased, thereby increasing energy dissipation, which is shared between the concrete and the PU coating, and thus, is deflected more. Furthermore, strain energy density was lower under impact condition than under quasi-static condition by factors of 0.88, 0.40, 0.33, and 0.33 for the uncoated specimen and the specimens coated with 1, 2, and 4 mm-thick PU, respectively, thereby demonstrating the convergence of this ratio with increasing coating thickness. Although the enhancement of the strain energy density of the specimens coated on the bottom face is higher than that of the specimens coated on the top face under quasi-static condition, the respective values are lower under impact condition. A similar behaviour was observed in strain enhancement as discussed earlier. Therefore, a conclusion can be drawn that the application of PU coating on the rear face contributes positively to enhancing the strain energy of concrete specimens, and that such enhancement increases with increasing PU layer thickness.

### 3.2.4. Failure mode and crack propagation profile

In terms of cracks during ultimate failure, only flexural cracks were formed and neither diagonal nor direct shear crack was observed similar to previous cases. Fig. 13 shows the crack propagation patterns formed in the specimens under both conditions. In
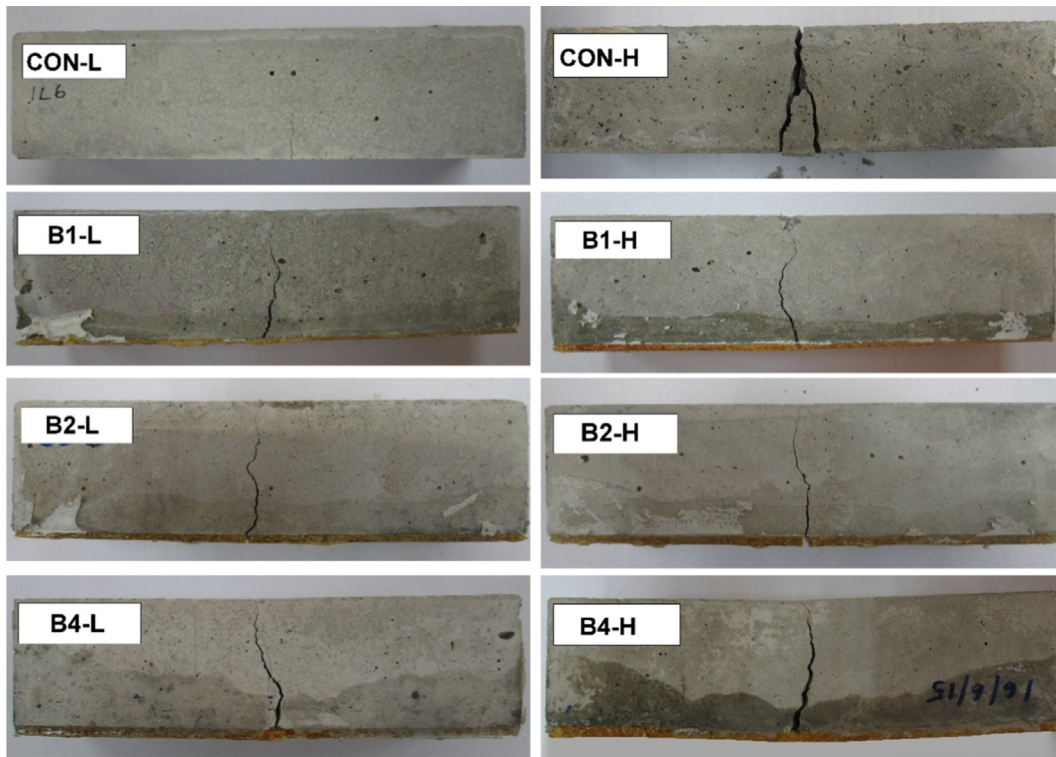
**Fig. 13.** The crack and crack propagation of the test specimens with bottom coating (T2-L, (T) coating face, (2) coating thickness, (L) strain rate condition).

all the cases, one major crack existed closest to the mid-span of the concrete specimens. The crack lines stretch fully across the bottom face. PU coatings were applied on the tension face of the concrete specimens; hence, the failure of the PU layers was found to have the same crack line of the concrete element shown in Fig. 14. All the cracks recorded under impact condition are wider than those recorded under quasi-static condition due to the drastic failure behaviour of concrete under impact conditions. Because concrete shows high fragmentation, with severe cracks (deeper and wider cracks) under high strain rate conditions than quasi-static condition. Although the PU layers failed, the coatings remained completely intact and still bonded well with concrete. The crack width on the bottom face of the test specimens increased with the increasing thickness of the PU coating because the coated element could have withstood higher strain when coating thickness was high. Visual examination shows that the PU resin wet the concrete surface well at the initial stage. In addition, scanning electron microscopy analysis showed that PU resin was able to penetrate through the porous structure within the concrete because of its low viscosity. The microscopic image of the interface between the concrete substrate (A) and PU resin (B) is shown in Fig. 15(a), which shows the spread of PU resin over the concrete substrate to make perfect contact with the uneven concrete surface. The

interaction of PU with the porous concrete within the concrete substrate is indicated in Fig. 15(b), which shows that the PU sprayed through the porous concrete well and gained additional confinement by spreading the polymer matrix within the concrete by bonding with cement and aggregates directly. This additional PU matrix within the concrete also provided an additional confinement effect for the concrete, which enhanced the toughness and strain capacities, and consequently enhance the tensile strength and flexural capacity of the material. Furthermore, the PU coating on the bottom face significantly enhanced the stability level of the concrete element even after the concrete element was cracked, since coating holds the broken concrete parts together and reduces fragmentation effect. Therefore, all the test specimens coated with PU on the rear face could sufficiently enhance their dynamic mechanical resistance in terms of stability and their capability to dissipate loads and pressure.

### 3.3. Coating on both faces

This section examines the influence of the thickness of the PU coating on both sides of the concrete element on dynamic resistivity. Specimens T1B1, T2B2, and T4B4 are combinations of specimens T1, T2, and T4 and B1, B2, and B4. T1B1, T2B2, and T4B4 were coated on both their top and bottom faces with 1, 2, and 4 mm-thick PU, respectively. Similar to the other test specimens, T1B1, T2B2, and T4B4 were subjected to two different strain rates, and their dynamic resistivity was observed and discussed as follows. The typical flexural stress–strain responses of the test specimens are shown in Fig. 16(a), which provides a comparison of the stress–strain curves of the uncoated and coated specimens under quasi-static and impact conditions. A significant difference in the mechanical response of the test specimens was observed with different coating thicknesses under both tested loading conditions. Similar to those in the previous sections, stiffness and ultimate stress were higher under impact condition than under
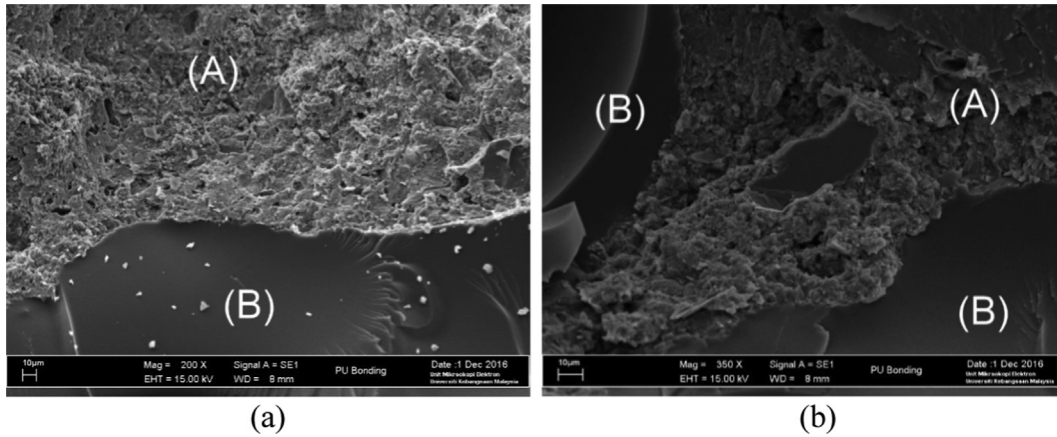


**Fig. 14.** The crack propagation of the test specimens on bottom face which contain PU layer on bottom face.

**Fig. 15.** The section of the interface of PU and concrete (a) interface between concrete substrate, (b) interaction of PU with porous concrete.

quasi-static condition, whereas deflection was lower. Under quasi-static condition, a similar observation was made on the stress–strain response of the test specimen coated on the bottom face. The stress–strain curve of the specimens coated with 1 mm- and



**Fig. 16.** The test specimens with top and bottom coatings (a) stress–strain (b) cumulative strain energy-strain: (T2-L, (T) coating face, (2) coating thickness, (L) strain rate condition).

2 mm-thick PU exhibited a sudden reduction in flexural strength after attaining a flexural strength that was slightly higher than the ultimate flexural strength of the uncoated specimen, in which the concrete sample cracked. This result shows that although the concrete specimen has cracked, the PU-coated specimens can still resist certain load and pressure up to significant strain level because the un-failed PU layer holds the cracked concrete elements together until the PU layer loses its structural capacity. However, this behaviour was not demonstrated by the specimen coated with 4 mm-thick PU on both sides, thereby showing that its ultimate failure occurred immediately before failure, which is dissimilar to the specimens with 1 mm and 2 mm thick coatings on both faces. Because the increase in thickness has resulted significant enhancement in the tensile capacity of concrete in the bottom face which can resist high strains. But, when concrete beam fails, it created a wide crack suddenly, and subsequently sudden enhancement of the tensile stress concentration, and subsequently enhancement in strain of PU along the crack line. Therefore, sudden failure of PU layer was shown while gap between the time of the failure of concrete and PU was not shown. The stiffness of the test specimens decreased with increasing coating thickness under both quasi-static and impact conditions, whereas a slight increase in ultimate flexural stress was exhibited
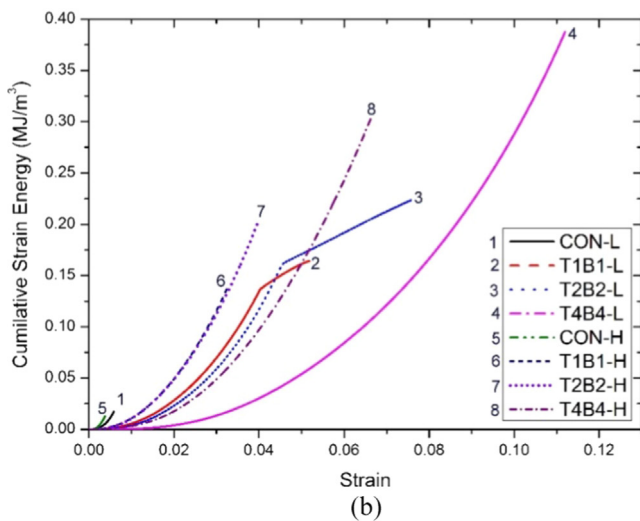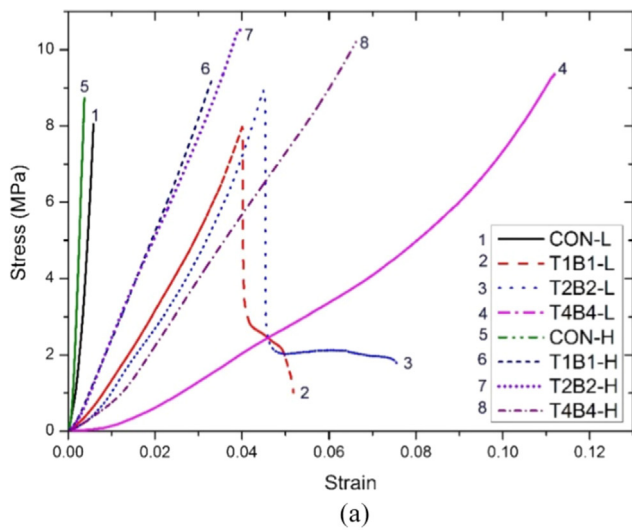
### 3.3.1. Ultimate flexural stress

The stress–strain responses showed that the specimens attained their ultimate flexural strength immediately before failure of concrete and before their ultimate failure. Under quasi-static condition, when a PU layer is applied on the rear face of a specimen, although the concrete specimen will crack, the un-failed PU layer can still resist certain load and pressure up to a significant strain level until it eventually cracks except type T4B4 as aforementioned, which highlights the requirement of proper control of the coating thickness. Under impact condition, all the test specimens in each test configuration attained ultimate flexural stress immediately before failure. The average ultimate flexural strengths of the test specimens are presented in Fig. 17(a). For each coating thickness, a higher ultimate flexural strength was observed under impact condition than under quasi-static condition. Unlike in the previous section, enhancement of the ultimate flexural stress under quasi-static condition was exhibited at 5% and 23% in the specimens coated with 2 mm- and 4 mm-thick PU compared with the uncoated specimen, whereas no enhancement was observed in the specimen coated with 1 mm-thick PU. The uncoated specimen attained its ultimate flexural stress immediately before failure, whereas those coated with 1 mm- and 2 mm-thick PU reached
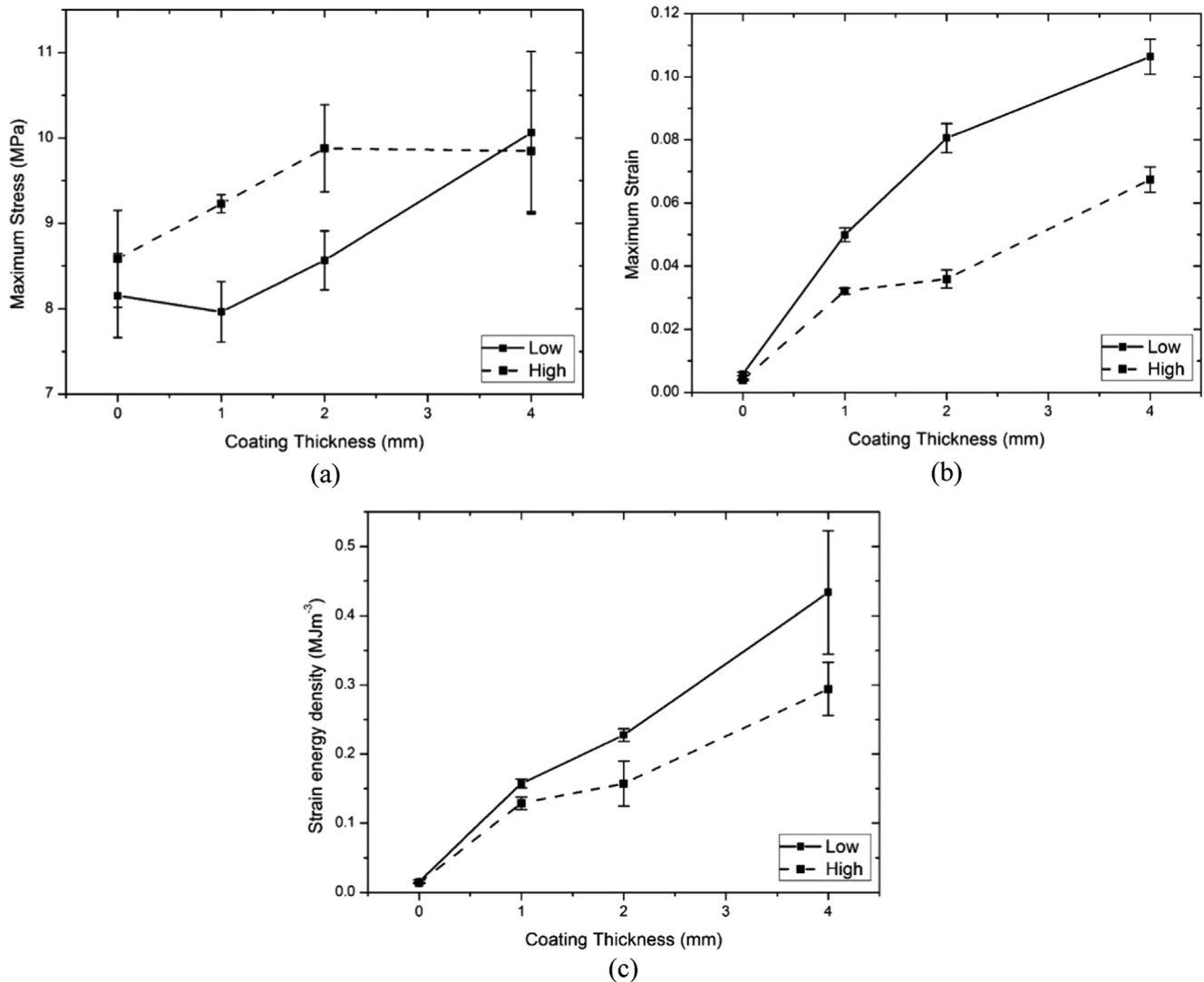
(a)



(b)



(c)

**Fig. 17.** The flexural properties of the test specimens with top and bottom coatings; (a) Ultimate flexural stress, (b) Failure strain, (c) Strain energy density at failure.

their ultimate failure after the concrete specimen was cracked, but the PU layer remained un-failed. However, when coating thickness on both sides was 4 mm, the ultimate flexural strength occurred immediately before failure, thereby indicating the simultaneous failure of the concrete specimen and the bottom PU layer. In addition, the maximum flexural stress was enhanced by 7.5%, 15%, and 15% compared with the uncoated specimen under impact condition.

*3.3.2. Failure strain*

Fig. 17(b) shows the plot of the relationship of the average strain during ultimate failure of the test specimens with coating thickness. The strain during ultimate failure of the test specimens increases with coating thickness under both quasi-static and impact conditions similar to the observation in the previous sections. Under quasi-static condition, the strain during ultimate failure exhibited by specimens T1B1, T2B2, and T4B4 was 8.5, 13.7, and 18.1 times that of the uncoated specimen (CON). Subsequently, enhancements of 8.0, 8.9, and 16.7 times were demonstrated under impact condition. Therefore, externally strengthened test specimens exhibited higher strain because of the elastomeric coating applied on both faces. This coating has high strain capacity, which enhances the strain capacity of the concrete

specimens because of the additional confinement effect provided by the PU matrix on both sides of the concrete element. Failure strain was lower under impact condition than under quasi-static condition by factors of 0.68, 0.64, 0.45, and 0.63 for the uncoated specimen and those coated with 1, 2, and 4 mm-thick PU, respectively. In the previous cases, the ratio of failure strain under impact and quasi-static conditions decreased with increasing coating thickness up to 10% compared with the thickness of the concrete specimen. A similar behaviour was observed, which exhibited a reduction of up to 10% of the coating layer. However, the ratio was increased when the coating layer thickness was 20% because of high enhancement of strain under impact condition compared with the 5% and 10%. Simultaneously, this result implies that a higher coating thickness provides higher deflection capability to the element, which reduce fragmentation, and withstand fragments through the coating, which are major causes of casualties. These observations indicate the stability of the PU-coated structural elements even after cracking and the effectiveness provided by coating thickness.

*3.3.3. Strain energy density*

The variations of cumulative strain energy with strain are presented in Fig. 16(b) under both quasi-static and impact conditions.
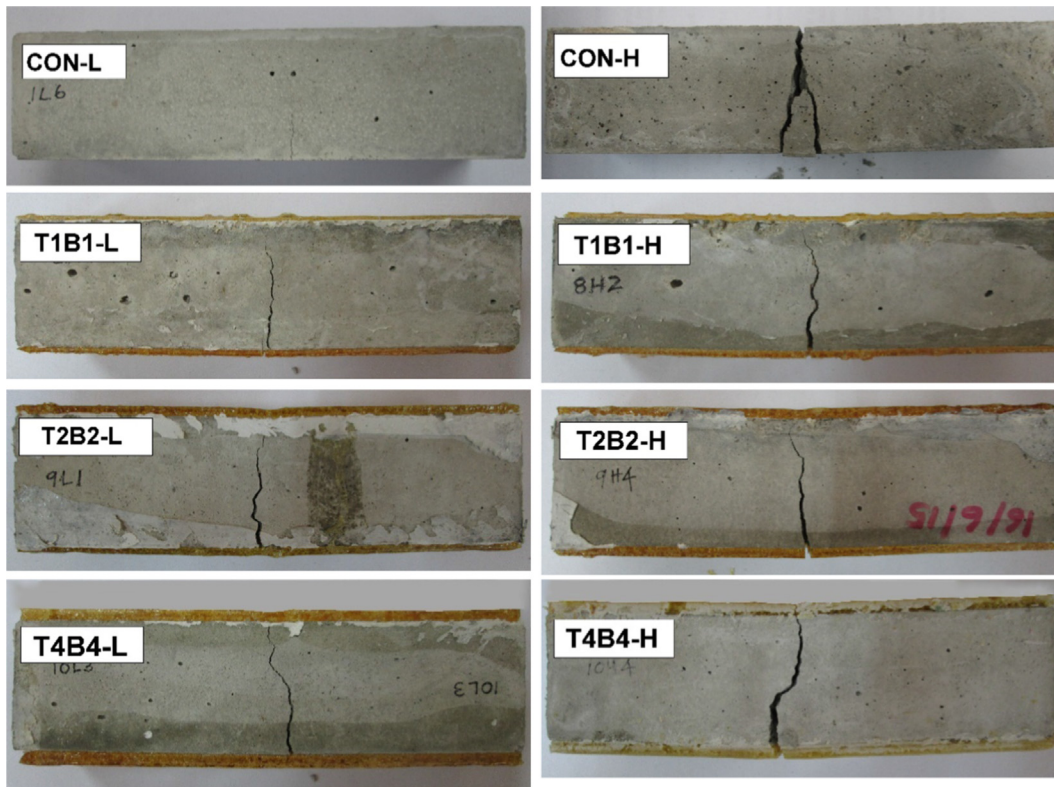
**Fig. 18.** The crack and crack propagation of the test specimens with coatings on both top and bottom faces (T2-L, (T) coating face, (2) coating thickness, (L) strain rate condition).

PU-coated test specimens exhibited higher strain energy density during ultimate failure because of the good energy dissipative capability of PU and the additional confinement effect in the concrete provided by the PU matrix within it. Fig. 17(c) compares the average strain energy densities during ultimate failure of different coating configurations under both quasi-static and impact conditions. Strain energy was enhanced by factors of 9.3, 11.3, and 21.2 under impact condition compared with the uncoated sample. This result is in good agreement with the current strengthening technique, which shows that strain energy absorption is considerably higher than that absorbed by the uncoated specimen. A lower enhancement was observed under impact condition than under quasi-static condition because of the strain rate sensitivity of PU and concrete. In particular, the strain energy during failure under impact condition is lower by factors of 0.88, 0.82, 0.69, and 0.68 compared with that under quasi-static condition for the uncoated specimen and those coated with 1, 2, and 4 mm-thick PU, respectively. These findings evidently show that the application of PU coating on both faces significantly enhances the strain
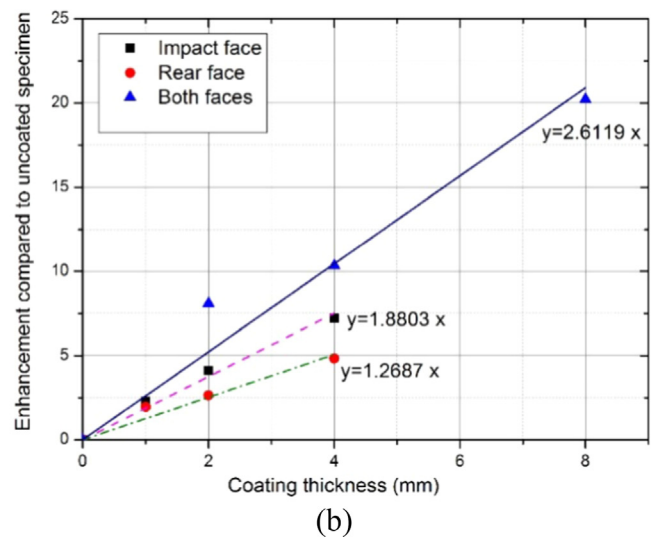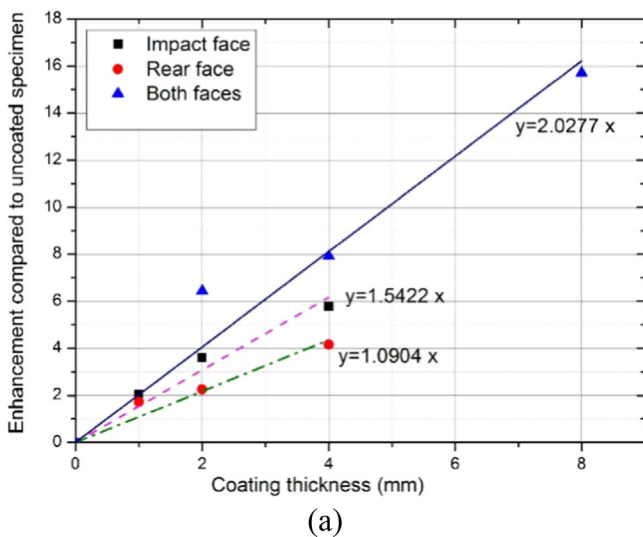


**Fig. 19.** The enhancements compared to uncoated specimen; (a) failure strain, and (b) ultimate strain energy density.

**Table 5**
Summary of the comparisons undertaken using PU coated concrete specimens.

| Coating location | Failure strain | | Strain energy density | |
|---|---|---|---|---|
| | Equation | $R^2$ | Equation | $R^2$ |
| Impact face | $y = 1.5422x$ | 0.9606 | $y = 1.8803x$ | 0.9852 |
| Rear face | $y = 1.0904x$ | 0.9484 | $y = 1.2687x$ | 0.9551 |
| Both faces | $y = 2.0277x$ | 0.9521 | $y = 2.6119x$ | 0.9583 |

energy capacity of concrete elements, which results in low kinetic energy, and subsequently, reduces the velocity of fragments.

### 3.3.4. Failure mode and crack propagation profile

The crack patterns formed on the specimens are presented in Fig. 18. The coating remained completely intact and still bonded well with the concrete even after the coated test specimens failed. Similarly, as discussed in the previous sections, one major crack, which was located closest to the mid-span of the test specimens, was observed in each test specimen. None of the evaluated specimens exhibited shear crack nor shear failure (neither diagonal nor direct shear). The PU layers on the top face of the concrete specimens were inspected and found undamaged. On the bottom face, the failure of the PU layers occurred along the same crack line of the concrete element. Except along the major flexural crack, the PU layers exhibited nearly no damage under both loading conditions in all the coating configurations. Crack length and crack width on the bottom face during ultimate failure of the test specimen increased with PU coating as observed in the previous sections because specimens deflected more at failure due to the enhancement of flexural capacity when coating thickness was higher. Debonding was not observed in any specimen; therefore, the thickness of the PU coating on both faces did not affect the debonding of PU.

According to the overall findings of the PU coated concrete specimens, significant enhancement was not shown in the ultimate flexural strength up to 2 mm thick coating (10% from beam depth) under impact condition. The enhancement in the ultimate flexural strength was about 10% when 4 mm PU coating (10% from beam depth) is applied on impact face or rear face, while 15% enhancement was shown when PU coating was applied on both faces with equal coating thickness. However, adding small thickness of PU coating has enhanced both failure strain, and ultimate strain energy density under impact condition. Enhancements of failure strain, and ultimate strain energy density compared to uncoated specimen are represented in linear correlations represents against coating thickness in Fig. 19(a), and Fig. 19(b) respectively. The equations and coefficient of determination, $R^2$, obtained for each property from the linear correlation of each property are indicated in Table 5. Application of coating on both faces provided the highest enhancement, while coating on rear face provides lowest enhancement. However, the coating location can be decide based on the applicability of PU coating on faces of real structures. Applicability of PU coating on a face depends on the factors such as the coating application location feasibility, and cost for the equipment, techniques, and expertise. As shown in Fig. 19 and in Table 5, a suitable coating location and coating thickness can be selected based on the expected and required enhancement in failure strain and strain energy density of concrete element.

### 4. Conclusions

This work investigated the flexural behaviour of elastomeric bio-based PU coated (unreinforced) concrete specimens with varying coating thicknesses and coating configurations under dynamic loading conditions (strain rates of 0.00033 s$^{-1}$ and 0.067 s$^{-1}$). The PU layer provided a positive effect to the behaviour of the speci-

mens, under both quasi-static and impact conditions; this technique provides higher strain capacity and strain energy density as well as marginal enhancement of ultimate flexural stress. Under impact conditions, with 4 mm thick coating (10% of total coating thickness compared to the total beam depth), a strength enhancement by a factor of 1.1, 1.1 and 1.15 can be achieved when PU coating is applied on impact face, rear face and both faces (with equal coating thickness) respectively. Also, the strain during ultimate failure can be enhanced by 6.8, 5.2, and 8.9 times with similar coating configuration as aforementioned. Accordingly, an enhancement of strain energy density of 8.2, 5.8, and 11.3 times were observed under impact condition compared with the uncoated concrete specimen. As the thickness of the PU layer was increased, the strain energy formed as a result of the enhanced strain work increases nearly linearly with PU layer thickness. Therefore, the strain energy density per unit thickness of the PU layer on either face can be used as a parameter to quantify the resistance of coated concrete specimens against impact loads. The enhancement of the failure strain and ultimate strain energy density can be presented as linear correlation with coating thickness, which the required coating thickness can be decide based on the expected enhancement in those properties. The overall enhancement was highest when the coating was provided on both faces, while coating on rear face provided the lowest enhancement under high strain rate condition. However, coating location can be decide based on the applicability of PU coating on faces of real structures. Debonding was not observed in any specimen, which implies better bond characteristics even under impact conditions, and the thickness of the PU layer on any face does not affect the debonding of PU. Even with minimum coating thickness (2.5%), drastic fragmentation effects can be reduced, as coating holds the broken concrete parts together. A conclusion can be drawn from these findings that the bio-based PU coating technique provides a feasible and sustainable solution for protecting concrete structures subjected to dynamic loads. The application of a bio-based PU layer (either on the impact face, rear face, or on both faces of the concrete specimens) increases dynamic resistance of a concrete element, which can be enhanced by increasing coating thickness on either side of the concrete element.

### CRediT authorship contribution statement

**H.M.C.C. Somarathna:** Conceptualization, Data curation, Formal analysis, Investigation, Methodology, Validation, Visualization, Writing - original draft, Writing - review & editing. **S.N. Raman:** Conceptualization, Data curation, Formal analysis, Funding acquisition, Investigation, Methodology, Project administration, Supervision, Validation, Writing - original draft, Writing - review & editing. **D. Mohotti:** Formal analysis, Investigation, Methodology, Writing - original draft. **A.A. Mutalib:** Conceptualization, Supervision, Validation. **K.H. Badri:** Formal analysis, Funding acquisition, Supervision.

## Declaration of Competing Interest

The authors declare that they have no known competing financial interests or personal relationships that could have appeared to influence the work reported in this paper.

## Acknowledgement

## References

[1] T. Krauthammer, Modern Protective Structures, 1st ed., CRC Press, Taylor & Francis Group, 2008.

[2] D. Cormie, G. Mays, P. Smith, Blast Effects on Buildings, Third Edition, ICE Publishing, 2019. doi:10.1680/beob.61477.

[3] H.M.C.C. Somarathna, S.N. Raman, A.A. Mutalib, K.H. Badri, Elastomeric polymers for blast and ballistic retrofitting of structures, J. Teknol. 76 (2015), https://doi.org/10.11113/jt.v76.3608.

[4] S. Das Adhikary, B. Li, K. Fujikake, N.D. Academy, Low velocity impact response of reinforced concrete beams: Experimental and numerical investigation, Int. J. Prot. Struct. 6 (2015) 81–112.

[5] S.N. Raman, Polymeric Coatings for Enhanced Protection of Reinforced Concrete Structures from the Effects of Blast PhD Thesis, Department of Civil and Environmental Engineering, The University of Melbourne, Australia, 2011.

[6] W. Tantrapongsaton, C. Hansapinyo, P. Wongmatar, T. Chaisomphob, FLEXURAL REINFORCED CONCRETE MEMBERS WITH MINIMUM REINFORCEMENT UNDER LOW-VELOCITY IMPACT LOAD, Int. J. GEOMATE. 14 (2018) 129–136.

[7] S. Khandelwal, K.Y. Rhee, Recent advances in basalt-fiber-reinforced composites: Tailoring the fiber-matrix interface, Compos. Part B Eng. (2020), https://doi.org/10.1016/j.compositesb.2020.108011 108011.

[8] M.Z. Naser, R.A. Hawileh, J.A. Abdalla, Fiber-reinforced polymer composites in strengthening reinforced concrete structures: A critical review, Eng. Struct. 198 (2019), https://doi.org/10.1016/j.engstruct.2019.109542 109542.

[9] G. Camata, E. Spacone, R. Zarnic, Experimental and nonlinear finite element studies of RC beams strengthened with FRP plates, Compos. Part B Eng. 38 (2007) 277–288, https://doi.org/10.1016/j.compositesb.2005.12.003.

[10] C. Part, E. Rc, F. Rc, T. Frp, Flexural behaviour of concrete beams reinforced with di ff erent grade steel and strengthened by CFRP strips, Compos. Part B Eng. 167 (2019) 411–421, https://doi.org/10.1016/j.compositesb.2019.02.056.

[11] G. Di Luccio, L. Michel, E. Ferrier, E. Martinelli, Seismic retro fi tting of RC walls externally strengthened by fl ax e FRP strips, Compos. Part B Eng. 127 (2017) 133–149, https://doi.org/10.1016/j.compositesb.2017.06.017.

[12] X. Kong, X. Qi, Y. Gu, I.A. Lawan, Y. Qu, Numerical evaluation of blast resistance of RC slab strengthened with AFRP, Constr. Build. Mater. 178 (2018) 244–253, https://doi.org/10.1016/j.conbuildmat.2018.05.081.

[13] S.H. Alsayed, H.M. Elsanadedy, Z.M. Al-Zaheri, Y.A. Al-Salloum, H. Abbas, Blast response of GFRP-strengthened infill masonry walls, Constr. Build. Mater. 115 (2016) 438–451, https://doi.org/10.1016/j.conbuildmat.2016.04.053.

[14] T. Yılmaz, N. Kıraç, Ö. Anil, R.T. Erdem, C. Sezer, Low-velocity impact behaviour of two way RC slab strengthening with CFRP strips, Constr. Build. Mater. 186 (2018) 1046–1063, https://doi.org/10.1016/j.conbuildmat.2018.08.027.

[15] K. Fujikake, S. Soeum, T. Matsui, CFRP strengthened RC beams subjected to impact loading, Procedia Eng. 210 (2017) 173–181, https://doi.org/10.1016/j.proeng.2017.11.063.

[16] C. Batuwitage, S. Fawzia, D. Thambiratnam, X. Liu, R. Al-Mahaidi, M. Elchalakani, Impact behaviour of carbon fibre reinforced polymer (CFRP) strengthened square hollow steel tubes: A numerical simulation, Thin-Walled Struct. 131 (2018) 245–257, https://doi.org/10.1016/j.tws.2018.06.033.

[17] D. Saini, B. Shafei, Investigation of concrete-filled steel tube beams strengthened with CFRP against impact loads, Compos. Struct. 208 (2019) 744–757, https://doi.org/10.1016/j.compstruct.2018.09.057.

[18] T.M. Pham, H. Hao, Review of concrete structures strengthened with FRP against impact loading, Structures. 7 (2016) 59–70, https://doi.org/10.1016/j.istruc.2016.05.003.

[19] R. Sen, L. Liby, G. Mullins, Strengthening steel bridge sections using CFRP laminates, Compos. Part B Eng. 32 (2001) 309–322.

[20] A.B. Elnagar, H.M. Afefy, A.T. Baraghith, M.H. Mahmoud, Experimental and numerical investigations on the impact resistance of SHCC-strengthened RC slabs subjected to drop weight loading, Constr. Build. Mater. 229 (2019), https://doi.org/10.1016/j.conbuildmat.2019.116866 116866.

[21] W. Fan, D. Shen, T. Yang, X. Shao, Experimental and numerical study on low-velocity lateral impact behaviors of RC, UHPFRC and UHPFRC-strengthened columns, Eng. Struct. 191 (2019) 509–525, https://doi.org/10.1016/j.engstruct.2019.04.086.

[22] G. Maddaloni, M. Di Ludovico, A. Balsamo, G. Maddaloni, A. Prota, Dynamic assessment of innovative retro fi t techniques for masonry buildings, Compos. Part B Eng. 147 (2018) 147–161, https://doi.org/10.1016/j.compositesb.2018.04.038.

[23] Y. Zhang, X. Li, Y. Zhu, X. Shao, Experimental study on flexural behavior of damaged reinforced concrete (RC) beam strengthened by toughness-improved ultra-high performance concrete (UHPC) layer, Compos. Part B Eng. 186 (2020), https://doi.org/10.1016/j.compositesb.2020.107834 107834.

[24] B. Wang, Y. Chen, H. Fan, F. Jin, Investigation of low-velocity impact behaviors of foamed concrete material, Compos. Part B Eng. 162 (2019) 491–499, https://doi.org/10.1016/j.compositesb.2019.01.021.

[25] H.M.C.C. Somarathna, S.N. Raman, D. Mohotti, A.A. Mutalib, K.H. Badri, The use of polyurethane for structural and infrastructural engineering applications: A state-of-the-art review, Constr. Build. Mater. 190 (2018) 995–1014, https://doi.org/10.1016/j.conbuildmat.2018.09.166.

[26] S.N. Raman, T. Pham, T. Ngo, P. Mendis, Experimental Investigation on the Behaviour of RC Panels Retrofitted with Polymer Coatings under Blast Effects, in: Proc. 2nd Int. Conf. Sustain. Built Environ., Kandy, Sri Lanka, 2012: p. 14 pgs.

[27] H.M.C.C. Somarathna, S.N. Raman, D. Mohotti, A.A. Mutalib, K.H. Badri, Rate dependent tensile behavior of polyurethane under varying strain rates, Constr. Build. Mater. 254 (2020), https://doi.org/10.1016/j.conbuildmat.2020.119203 119203.

[28] D. Mohotti, T. Ngo, P. Mendis, S.N. Raman, Polyurea coated composite aluminium plates subjected to high velocity projectile impact, Mater. Des. 52 (2013) 1–16, https://doi.org/10.1016/j.matdes.2013.05.060.

[29] J.S. Davidson, J.R. Porter, R.J. Dinan, M.I. Hammons, J.D. Connell, Explosive testing of polymer retrofit masonry walls, J. Perform. Constr. Facil. 18 (2004) 100–106, https://doi.org/10.1061/(ASCE)0887-3828(2004)18:2(100).

[30] J. Fan, A. Chen, Studying a flexible polyurethane elastomer with improved impact-resistant performance, Polymers (Basel) 11 (2019), https://doi.org/10.3390/polym11030467.

[31] J. Zhang, W. Tu, Z. Dai, Synthesis and characterization of transparent and high impact resistance polyurethane coatings based on polyester polyols and isocyanate trimers, Prog. Org. Coat. 75 (2012) 579–583, https://doi.org/10.1016/j.porgcoat.2012.05.005.

[32] H.M.C.C. Somarathna, S.N. Raman, A.A. Mutalib, K.H. Badri, Tensile Behavior of Polyurethane under Low to Intermediate Strain Rates, in: 13th Int. Conf. Concr. Eng. Technol. 2016, Selangor, Malaysia, 2016: p. 6 pgs.

[33] D. Mohotti, T. Ngo, S.N. Raman, M. Ali, P. Mendis, Plastic deformation of polyurea coated composite aluminium plates subjected to low velocity impact, Mater. Des. 56 (2014) 696–713, https://doi.org/10.1016/j.matdes.2013.11.063.

[34] J.S. Davidson, S. Sudame, DEVELOPMENT OF COMPUTATIONAL MODELS AND INPUT SENSITIVITY STUDY OF POLYMER REINFORCED CONCRETE MASONRY WALLS SUBJECTED TO BLAST, 140 Hoehn Building, 1075 13th Street South Birmingham, AL 35294-4440, 2004.

[35] J.S. Davidson, J.W. Fisher, M.I. Hammons, J.R. Porter, R.J. Dinan, Failure Mechanisms of Polymer-Reinforced Concrete Masonry Walls Subjected to Blast, J. Struct. Eng. 131 (2005) 1194–1205.

[36] Y. Wang, M. Xu, C. Yang, M. Lu, J. Meng, Z. Wang, M. Wang, Effects of elastoplastic strengthening of gravel soil on rockfall impact force and penetration depth, Int. J. Impact Eng. 136 (2020), https://doi.org/10.1016/j.ijimpeng.2019.103411 103411.

[37] Y. Yuan, S. Wang, P. Tan, H. Zhu, Mechanical performance and shear constitutive model study of a new high-capacity polyurethane elastomeric bearing, Constr. Build. Mater. 232 (2020), https://doi.org/10.1016/j.conbuildmat.2019.117227 117227.

[38] T.L. Attard, L. He, H. Zhou, Improving damping property of carbon-fiber reinforced epoxy composite through novel hybrid epoxy-polyurea interfacial reaction, Compos. Part B Eng. 164 (2019) 720–731, https://doi.org/10.1016/j.compositesb.2019.01.064.

[39] Y.a. Bahei-El-Din, G.J. Dvorak, Enhancement of blast resistance of sandwich plates, Compos. Part B Eng. 39 (2008) 120–127, https://doi.org/10.1016/j.compositesb.2007.02.006.

[40] Z. Liu, H. Chen, Deformation mechanism and failure-tolerant characteristics of polymer-coated sheet metal, Integr. Med. Res. (2020), https://doi.org/10.1016/j.jmrt.2020.02.017.

[41] M.R. Amini, J. Isaacs, S. Nemat-Nasser, Investigation of effect of polyurea on response of steel plates to impulsive loads in direct pressure-pulse experiments, Mech. Mater. 42 (2010) 628–639, https://doi.org/10.1016/j.mechmat.2009.09.008.

[42] M.R. Amini, J.B. Isaacs, S. Nemat-Nasser, Experimental investigation of response of monolithic and bilayer plates to impulsive loads, Int. J. Impact Eng. 37 (2010) 82–89, https://doi.org/10.1016/j.ijimpeng.2009.04.002.

[43] K. Ackland, C. Anderson, T.D. Ngo, T. Duc, Deformation of polyurea-coated steel plates under localised blast loading, Int. J. Impact Eng. 51 (2013) 13–22, https://doi.org/10.1016/j.ijimpeng.2012.08.005.

[44] M. Grujicic, B. Pandurangan, B. d'Entremont, The role of adhesive in the ballistic/structural performance of ceramic/polymer–matrix composite hybrid armor, Mater. Des. 41 (2012) 380–393, https://doi.org/10.1016/j.matdes.2012.05.023.

[45] M.S. Hoo Fatt, X. Ouyang, R.J. Dinan, Blast Response of Walls Retrofitted with Elastomer Coatings., in: Struct. under Shock Impact VIII Proc. 8th Int. Conf. Struct. under Shock Impact., Crete, Greece, 2004: pp. 129–138.

[46] J.T. Baylot, F. Asce, B. Bullock, M. Asce, T.R. Slawson, S.C. Woodson, Blast response of lightly attached concrete masonry unit walls, J. Struct. Eng. (2005) 1186–1193, https://doi.org/10.1061/~ASCE!0733-9445~2005!131:8~1186!.

[47] T. Hrynyk, J.J. Myers, Comparing slenderness effects on the out-of-plane behavior of URM infills using modern retrofits, in: Fourth Int. Conf. FRP Compos. Civ. Eng., Zurich, Switzerland, 2008: pp. 22–24.

[48] J. Wang, H. Ren, X. Wu, C. Cai, Blast response of polymer-retrofitted masonry unit walls, Compos. Part B Eng. 128 (2017) 174–181, https://doi.org/10.1016/j.compositesb.2016.02.044.

[49] D. Mohotti, M. Ali, T. Ngo, J. Lu, P. Mendis, D. Ruan, Out-of-plane impact resistance of aluminium plates subjected to low velocity impacts, Mater. Des. 50 (2013) 413–426, https://doi.org/10.1016/j.matdes.2013.03.023.

[50] L. Xue, W. Mock, T. Belytschko, Mechanics of Materials Penetration of DH-36 steel plates with and without polyurea coating, Mech. Mater. 42 (2010) 981–1003, https://doi.org/10.1016/j.mechmat.2010.08.004.

[51] M. Duda, J. Pach, G. Lesiuk, Influence of polyurea composite coating on selected mechanical properties of AISI 304 steel, Materials (Basel) 12 (2019) 1–13, https://doi.org/10.3390/ma12193137.

[52] Y.a. Bahei-El-Din, G.J. Dvorak, Wave propagation and dispersion in sandwich plates subjected to blast loads, Mech. Adv. Mater. Struct. 14 (2007) 465–475, https://doi.org/10.1080/15376490701298975.

[53] G.J. Dvorak, Y.A. Bahei-el-din, A.P. Suvorov, Impact and blast resistance of sandwich plates, major accompl, Compos. Mater. Sandw. Struct. (2009) 625–659, https://doi.org/10.1007/978-90-481-3141-9_24.

[54] N. Saba, M. Jawaid, O.Y. Alothman, M.T. Paridah, A review on dynamic mechanical properties of natural fibre reinforced polymer composites, Constr. Build. Mater. 106 (2016) 149–159, https://doi.org/10.1016/j.conbuildmat.2015.12.075.

[55] R.G. Crookes, H. Wu, S.J. Martin, C. Kay, G.W. Critchlow, Bio-inspired platelet reinforced elastomeric-ceramic composites for impact and high strain rate applications, Compos. Sci. Technol. 184 (2019), https://doi.org/10.1016/j.compscitech.2019.107857 107857.

[56] S.N. Raman, M. Jamil, T. Ngo, P. Mendis, T. Pham, Retrofitting of RC panels subjected to blast effects using elastomeric polymer coatings, in: Concr. Solut. - Proc. Concr. Solut. 5th Int. Conf. Concr. Repair, Belfast, Northern Ireland, 2014: pp. 353–360. doi:10.1201/b17394-55.

[57] S. Parniani, H. Toutanji, Monotonic and fatigue performance of RC beams strengthened with a polyurea coating system, Constr. Build. Mater. 101 (2015) 22–29, https://doi.org/10.1016/j.conbuildmat.2015.10.020.

[58] N. Iqbal, P.K. Sharma, D. Kumar, P.K. Roy, Protective polyurea coatings for enhanced blast survivability of concrete, Constr. Build. Mater. 175 (2018) 682–690, https://doi.org/10.1016/j.conbuildmat.2018.04.204.

[59] H.M.C.C. Somarathna, S.N. Raman, K.H. Badri, A.A. Mutalib, D. Mohotti, S. Engineering, S.D. Ravana, Quasi-static behavior of palm-based elastomeric polyurethane: for strengthening application of Structures under impulsive loadings, Polymers (Basel) 8 (2016) 20, https://doi.org/10.3390/polym8050202.

[60] H.M.C.C. Somarathna, S.N. Raman, D. Mohotti, A.A. Mutalib, K.H. Badri, Hyper-viscoelastic constitutive models for predicting the material behavior of polyurethane under varying strain rates and uniaxial tensile loading, Constr. Build. Mater. 236 (2020), https://doi.org/10.1016/j.conbuildmat.2019.117417 117417.

[61] H.M.C.C. Somarathna, S.N. Raman, A.A. Mutalib, K.H. Badri, Analysis of Strain Rate Dependent Tensile Behaviour of Polyurethanes, in: Proc. Int. Conf. Struct. Eng. Constr. Manag., Kandy, Sri Lanka, 2015: p. 7 pgs.

[62] H.M.C.C. Somarathna, S.N. Raman, A.A. Mutalib, K.H. Badri, Mechanical Characterization of Polyurethane Elastomers: For Retrofitting Application against Blast Effects, in: Proceedins Third Conf. Smart Monit. Assess. Rehabil. Struct. (SMAR 2015), Antalya, Turkey, 2015: pp. 82–89.

[63] S.N. Raman, H.M.C.C. Somarathna, A.A. Mutalib, K.H. Badri, M.R. Taha, Bio-Based Polyurethane Elastomer for Strengthening Application of Concrete Structures Under Dynamic Loadings, in: Int. Congr. Polym. Concr. (ICPIC 2018), Springer International Publishing, Cham, 2018: pp. 751–757. doi:10.1007/978-3-319-78175-4_96.

[64] S.N. Raman, H.M.C.C. Somarathna, A.A. Mutalib, K.H. Badri, Elastomeric polyurethane for retrofitting application of concrete structures under dynamic loadings, Adv. Constr. Mater. Syst. 2 (2017) 549–556.

[65] American Concrete Institute, Concrete Mix Design Full Peocedure ACI 211, United States, 2002.

[66] ASTMC39, ASTM C-39, in: Stand. Test Method Compressive Strength Cylind. Concr. Specimens, ASTM International, West Conshohocken, PA, 2014. www.astm.org.

[67] K. Haji, Biobased polyurethane from palm kernel oil-based polyol, Polyurethane (2012) 447–470, https://doi.org/10.5772/47966.

[68] ASTM C293/C293M - 16 Standard Test Method for Flexural Strength of Concrete (Using Simple Beam With Center-Point Loading), in: ASTM Int., West Conshohocken, PA, 2016. www.astm.org.

[69] S. Das Adhikary, B. Li, K. Fujikake, State-of-the-art review on low-velocity impact response of reinforced concrete beams, Mag. Concr. Res. 68 (2016).

[70] M. Johansson, Structural Behaviour in Concrete Frame Corners of Civil Defence Shelters, Non-linear Finite Element Analyses and Experiments, Chalmers University of Technology; Goteborg, Sweden, 2000.

[71] J. Eibl, B. Schmidt-Hurtienne, Strain-rate-sensitive constitutive law for concrete, J. Eng. Mech. 125 (1999) 1411–1420, https://doi.org/10.1061/(ASCE)0733-9399(1999)125:12(1411).

[72] R.C. Hibbeler, Mechanics of Materials, Pearson-Prentice Hall: Singapore, 2011. doi:10.1017/CBO9781107415324.004.

[73] S.N. Raman, T. Ngo, J. Lu, P. Mendis, Experimental investigation on the tensile behavior of polyurea at high strain rates, Mater. Des. 50 (2013) 124–129, https://doi.org/10.1016/j.matdes.2013.02.063.